IOPscience iopscience.iop.org

Home Search Collections Journals About Contact us My IOPscience

The effect of thermal annealing on crystallization in a-Si:H/SiO_2 multilayers by using layer by layer plasma oxidation

This article has been downloaded from IOPscience. Please scroll down to see the full text article.

2003 J. Phys.: Condens. Matter 15 5793

(http://iopscience.iop.org/0953-8984/15/34/309)

View the table of contents for this issue, or go to the journal homepage for more

Download details:
IP Address: 171.66.16.125
The article was downloaded on 19/05/2010 at 15:06

Please note that terms and conditions apply.

J. Phys.: Condens. Matter **15** (2003) 5793–5799 PII: S0953-8984(03)62628-7

The effect of thermal annealing on crystallization in a-Si:H/SiO_2 multilayers by using layer by layer plasma oxidation

Yanping Sui, Xinfan Huang[1]**, Zhongyuan Ma, Wei Li, Feng Qiao, Kai Chen and Kunji Chen**

National Laboratory of Solid State Microstructures and Department of Physics, Nanjing University, Nanjing 210093, People's Republic of China

E-mail: xfhuang@netra.nju.edu.cn

Received 23 April 2003
Published 15 August 2003
Online at stacks.iop.org/JPhysCM/15/5793

Abstract

Two post-treatments consisting of rapid thermal annealing (RTA) and furnace annealing (FA) were used to crystallize a-Si:H sublayers in a-Si:H/SiO_2 multilayers fabricated by alternate plasma-enhanced chemical vapour deposition of a-Si:H layers and plasma oxidation. Raman measurements show that the crystallization process of a-Si:H sublayers strongly depends on the post-treatment process. RTA is advantageous for nucleation, in which the size of the nuclei increases with higher annealing temperatures, and the crystalline volume ratio increases with longer annealing times. In FA, however, higher temperatures are required for further crystallization such as increasing the grain size and crystalline volume ratio. The ultimate size of nc-Si grains can be accurately determined by the thickness of the a-Si:H sublayer. Moreover, the mechanism of the constrained crystallization will also be discussed in accordance with the thermodynamic theory.

1. Introduction

There has been intense research into developing low-dimensional Si nanostructures for applications in Si-based optoelectronics. Efficient photoluminescence has been observed from porous Si [1] and Si nanoparticles, which were prepared by various methods, such as Si^+ ion implantation into SiO_2 layer [2], low-pressure chemical vapour deposition [3], magnetron sputtering [4] and amorphous Si (a-Si) deposition/recrystallization etc. Among the many methods of fabricating nc-Si, the thermal crystallization of a-Si/a-SiN_x:H [5] or a-Si/SiO_2 [6] layered structures shows great potential since the size of nc-Si grains can be precisely controlled and the surface can be effectively passivated, based on the constrained growth of nc-Si when

[1] Author to whom any correspondence should be addressed.

0953-8984/03/345793+07$30.00 © 2003 IOP Publishing Ltd Printed in the UK

the a-Si layer is ultrathin. The process of nucleation and growth of nc-Si from the amorphous phase in an ultrathin layer is quite different from that of bulk silicon. The mechanism of the constrained growth of nc-Si has been studied in accordance with classical thermodynamic theory.

In our previous work, the post-treatment methods of laser-induced and thermal annealing were adopted to fabricate nc-Si crystalline grains within a-SiN_x/a-Si:H multilayers. Visible and stable photoluminescence and electroluminescence have been observed at room temperature from the nc-Si grains [5, 7]. There is a strong correlation between the luminescence properties and the structure of the nc-Si grains formed by the post-treatment processing. However, the influence of thermal annealing on the interior structure of an ultrathin a-Si sublayer in the crystallization process has been reported less systemically. In this paper, we attempt to fabricate a-Si:H/SiO_2 multilayers by silicon deposition and *in situ* plasma oxidation, and to crystallize a-Si:H layers using a rapid thermal process and furnace annealing (FA). Raman scattering spectroscopy was utilized to investigate the amorphous-to-crystalline evolution of the a-Si:H/SiO_2 multilayers during thermal treatment. It is found that the Raman phonon band shifts with the variation of annealing time and temperature, which can be interpreted within the crystalline thermodynamic theory. Finally, the detailed local structure change in the annealing process is also described.

2. Experiments

a-Si:H/SiO_2 multilayers with 14 and 40 periods were fabricated on fused quartz at 250 °C by silicon deposition and layer by layer plasma oxidation in a computer-controlled plasma-enhanced chemical vapour deposition (PECVD) system [8]. The deposition of silane was carried out at 260 mTorr under a rf power of 50 W. The *in situ* plasma oxidation was realized by using pure oxygen gas at 280 mTorr with an rf power of 50 W. The thickness of the a-Si sublayer is 6 nm and the thickness of the SiO_2 sublayer in the two samples is 12 and 2 nm, respectively. The crystallization of the a-Si:H sublayer was performed by two kinds of post-treatment, namely RTA, and RTA followed by FA. The annealing temperature of RTA varies from 800 to 1000 °C. RTA is carried out at an increase rate of about 100 °C s^{-1}. In the FA process the temperature was set at 1000 and 1100 °C. FA is carried out at an increase rate of about 10 °C min^{-1} to the set values. All annealing steps were performed in a N_2 atmosphere.

The crystallinity of the annealed samples and the change in structure after thermal annealing were verified by Raman spectroscopy using the 514.5 nm line of an Ar^+ laser in a JY T64000. The microstructures of the annealed samples are revealed by cross-section transmission electron microscopy (TEM) measurements with a JEM200CX microscope working at 200 kV.

3. Results and discussion

Figure 1 shows the Raman spectra of the unannealed sample and the samples after RTA at different temperatures for the same time of 100 s. The Raman spectrum with the TO mode at 480 cm^{-1} of the unannealed sample shows the feature of amorphous Si. The a-Si-like band is still present in the Raman spectrum of the sample annealed at 900 °C. But the narrowed and slightly downshifted Raman band indicates that the structure of the a-Si sublayers annealed at 900 °C is different from that of the unannealed sample, which shows the network of a-Si becoming more disordered [9]. Raman spectra of the samples annealed at 900 °C indicate the formation of nc-Si in ultrathin a-Si sublayers with sharp TO phonon peaks at 514–516.5 cm^{-1}.

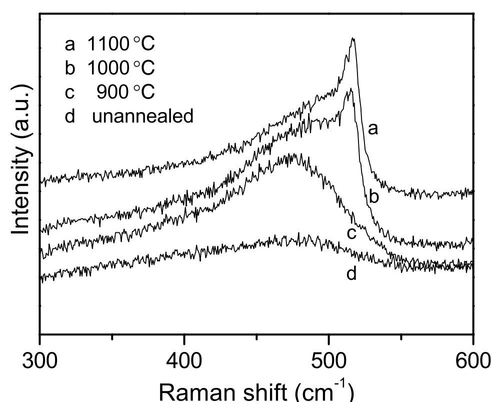

Figure 1. Raman spectra of the samples before and after RTA for 100 s at different temperatures, with a Si sublayer thickness of 6 nm and a SiO_2 sublayer thickness of 12 nm.

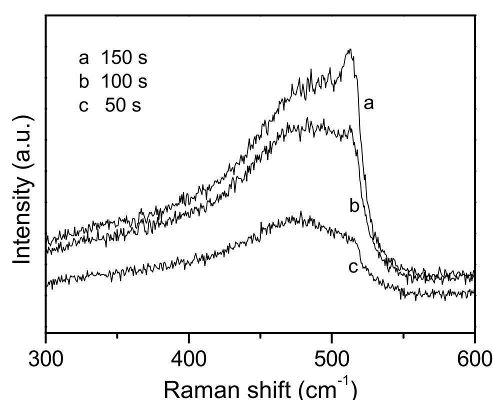

Figure 2. Raman spectra of the samples after RTA at 1000 °C for different annealing times, with a Si sublayer thickness of 6 nm and a SiO_2 sublayer thickness of 2 nm.

According to the phonon confinement effect, the upshift of the phonon peak in the sample annealed at 1100 °C is due to the fact that the nc-Si grains are larger than those of the sample annealed at 1000 °C. Above all, it is found that there is a threshold temperature of crystallization in the a-Si:H/SiO_2 multilayers with an a-Si sublayer thickness of 6 nm, which should be in the range of 900–1000 °C.

We investigated the effect of different annealing time on the crystallinity of samples annealed above threshold temperature. Figure 2 shows the Raman spectra of the samples annealed at the same temperature of 1000 °C for different times in the range 50–150 s. The c-Si-like band can be clearly seen although the signal in the spectrum of the sample annealed for 50 s is very weak compared with other samples. It is seen that significant changes occur in the c-Si-like TO region with increased annealing time. The crystalline volume ratio was also quantified from the definition: $X_c = I_c/(I_c + 0.88I_a)$, where I_c and I_a are the integrated areas of the TO bands of nc-Si and a-Si respectively, and the factor 0.88 [10] is the ratio of the Raman efficiencies for crystalline and amorphous Si. The crystalline fraction increases monotonously from 23 to 39% in the samples with annealing times from 50 to 150 s.

Above the threshold temperature, crystallization becomes observable from the emergence of a sharp c-Si-like Raman peak. In addition, the crystalline Raman peaks become more

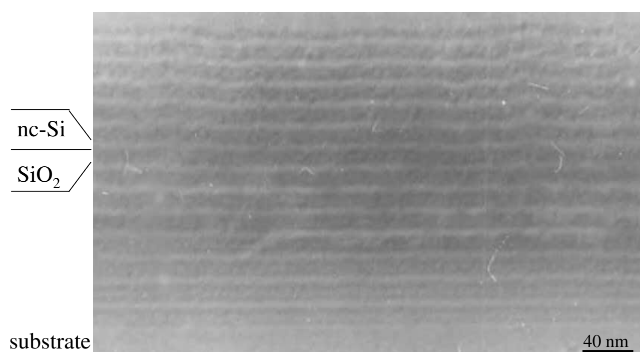

Figure 3. The cross-section TEM micrograph of the sample with 6 nm-thick a-Si sublayers and 12 nm-thick SiO_2 sublayers after FA following RTA.

prominent with increasing annealing time and temperature. It is significant that both the crystalline fraction and the size of the nc-Si grains increase with the rise in temperature, as shown in figure 1. There was a slight shift of the c-Si-like TO peak position with the protraction of annealing time at 1000 °C, whereas the crystalline fraction of the sample annealed for 150 s has increased by 17% over that of the sample for 50 s, as shown in figure 2. This can be explained by the thermodynamic theory. RTA is a process that leads to nucleation in a short time since the rise in temperature is rapid. When the external energy exceeds the crystallization threshold energy, the a-Si:H layers become inhomogeneous due to the drastic variance in temperature. Thus some Si atoms may obtain more energy than others, and when there is enough energy to overcome the nucleation barrier these atoms conglomerate to form nuclei. The higher the energy of storage during a rapid process, the larger the nc-Si grains will become during the incipient nucleation stage. However, if the nucleation energy is provided by sustained annealing at steady temperature, more nuclei will appear in an a-Si layer, so the nucleation density will increase. In the comparatively short-lived duration of RTA, the extension of RTA time produces more nuclei, but the size of the nuclei will not change. Therefore, the size of the nuclei depends on the RTA temperature, and the nucleus density is determined by the annealing time at the RTA temperature.

Since high-temperature and long-time annealing can release the strain in nc-Si/SiO_2 multilayer and decrease the interface defect density of Si/SiO_2 [6], we studied annealing processes of FA following RTA. The size and crystallinity of nc-Si grains formed in the FA process were also increased. Figure 3 shows the cross-section TEM micrograph of the sample with 6 nm-thick a-Si sublayers and 12 nm-thick SiO_2 sublayers annealed after FA at 1100 °C for 1 h. One can see that the nc-Si formed is embedded within the initial a-Si sublayers. The flat and abrupt interface between a-Si and SiO_2 remains after two steps of thermal annealing. Besides the TEM analysis, the formation of a nc-Si/SiO_2 multilayer by two sequential steps of thermal annealing was testified by Raman scattering spectroscopy. Figure 4 shows the Raman spectra of the samples annealed by FA for 1 h at 1000 and 1100 °C following RTA at 1000 °C for 100 s. The c-Si-like bands dominate the spectra. In order to analyse the local microstructure of the Si after the FA process, we fit the Raman bands with Gaussian curves in figure 4 parts (2) and (3). It is seen that the Raman spectrum is composed of four latent bands [11], which are located at 400 cm^{-1} (LO mode of a-Si), 480 cm^{-1} (TO mode of a-Si), 520 cm^{-1} (TO mode of nc-Si), and 495–508 cm^{-1} (which is related to the expansion of the bond angle). According to the constraint crystallization theory, the Raman band of 495–508 cm^{-1} originates from the

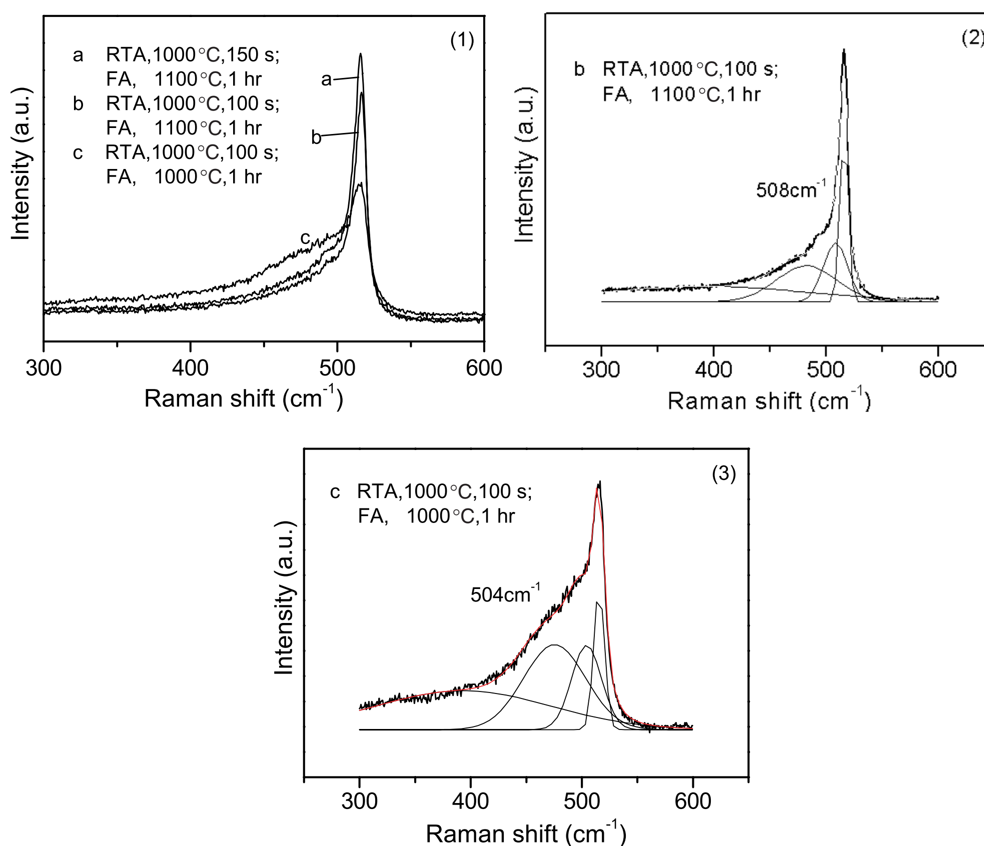

Figure 4. (1) Raman spectra of the samples after FA for 1 h at 1000 or 1100 °C following RTA shown in figure 1. Figure 4(2) and (3) show Raman spectra fitted by Gaussian curves.
(This figure is in colour only in the electronic version)

TO mode of small nc-Si grains that emerged in the FA process [12], which will be discussed later.

Table 1 lists the crystalline volume ratios of the samples after RTA, and after FA following RTA. It can be seen that under the same RTA conditions, the crystalline fraction of samples for FA at 1100 °C is higher than that for FA at 1000 °C. The shapes of the Raman bands of the samples annealed at 1100 °C are very similar despite the different times for RTA (see figure 4 curves (a), (b)). On the whole, the TO peak positions of all the FA samples are fixed in the range of 515.1–516.0 cm^{-1}. Based on the correlation length model [13], the size of the nc-Si grains are calculated to be in the range 4.2–4.5 nm. Exclusive of the dimensions of the interface extension, the grain size of the nc-Si formed in the FA process is close to the thickness of a-Si sublayer, which reflects the characteristic of constrained growth in the ultrathin Si layer located between two SiO_2 sublayers. When the annealing time is extended to 3 h, the Raman bands of all the samples are in line with those of samples annealed for 1 h, other than a slight increase in crystalline volume ratio.

When the size of Si crystallites is below 4 nm, the correlation length model does not give a satisfactory description of the Raman band-shape consistent with the real size of the nc-Si grains. According to the model of Zi *et al* [14]: $\Delta\omega(D) = -A(a/D)^{\gamma}$, where $\Delta\omega(D)$ is the

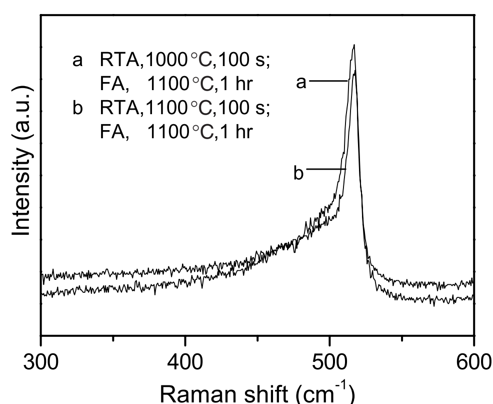

Figure 5. Raman spectra of the samples after FA for 1 h at 1100 °C following RTA shown in figure 2.

Table 1. Crystalline volume ratios (CVRs) of the samples in figure 4 after RTA, and FA following RTA.

		FA condition			
	CVR	No FA	1000 °C, 1 h	1100 °C, 1 h	1100 °C, 3 h
RTA	1000 °C, 100 s	32.0%	46.6%	60%	63%
condition	1000 °C, 150 s	39.4%		61%	63%

Raman shift in a nanocrystal with diameter D, a is the lattice constant of Si ($a = 0.543$ nm), $A = 47.41$ cm^{-1} and $\gamma = 1.44$ are fit parameters that describe the phonon confinement in nanometric spheres of diameter D. The fourth Raman band situated in the range 495–508 cm^{-1} is related to the small nc-Si grains with sizes around 1 nm. It indicates that some new, small nuclei emerge from the sequential FA process.

Figure 5 is the Raman spectra of the samples annealed by FA at 1100 °C for 1 h following RTA at temperatures of 1000 and 1100 °C respectively, shown in figure 1. The features of the Raman band of the sample with RTA at 1000 °C resemble that of the sample with RTA at 1100 °C. The average size of a nc-Si grain is 4.7 nm, based on the correlation length model which is in accord with the thickness of a-Si sublayer. Though the size of nuclei formed by RTA at 1100 °C is greater than that of the nuclei formed by RTA at 1000 °C, the ultimate size of the nc-Si grains formed after the FA process tend to be identical to the thickness of the Si sublayers.

How do we explain the experimental results in the FA process? On the basis of thermodynamic theory, FA is a quasi-equilibrium process in which the energy is uniformly distributed in the Si sublayers. So Si atoms around the former nuclei need less energy to conglomerate, without overcoming the nucleation barrier. After the nucleation process is finished by RTA, the nuclei will grow up to be nc-Si grains in the FA process. When an nc-Si grain has grown to a certain size, its growth will be constrained by the interface between the silicon and the silicon oxide. From the thermodynamic theory, Zhang *et al* [15] analyse the constrained growth of nc-Si quantitatively. It has been shown that in the process of nucleation and growth of nc-Si, the free energy change $\Delta G(r)$ can be considered as a criterion for constrained crystallization, and the growth of nc-Si always halts when $r > d/2$ (d is the thickness of the a-Si layer). The ultimate size may be considered to be the thermodynamic

equilibrium size. After the growth of nc-Si halts, the new nc-Si nuclei will appear in the FA process. The latter nuclei will appear only in the space of residual a-Si around the former nc-Si grains, so they are smaller than those that formed during the first stage. The size of the small nc-Si grains is only about 1 nm in our experiment.

4. Conclusions

In summary, we have prepared a-Si/SiO_2 multilayers by PECVD and *in situ* plasma oxidation. The thermal annealing crystallization of RTA followed by FA has been used to fabricate nc-Si within a-Si/SiO_2 multilayers. Raman spectra were utilized to analyse the microstructure of the samples during the nucleation and growth processes with different annealing times and temperatures. It is found that above the crystallization temperature, the size of the nuclei increases with higher annealing temperatures and the crystalline volume ratio increases with longer annealing times in the RTA process. Combining the results of the cross-section TEM and the Raman measurements, we think that size-controlled nc-Si can be prepared after two successive thermal annealing processes on account of the confinement of the interfaces. The mechanism of the constrained crystallization has been studied on the basis of thermodynamic theory. The interfacial free energy plays an important role in the process of constrained crystallization.

Acknowledgments

We would like to give special thanks to Professor Xiaoning Zhao and Jiancang Shen of NJU for TEM and Raman observations. The authors would also like to acknowledge the support of the State Key Program for Basic Research of China (grant No 2001 CB 610503); the National Nature Science Foundation of China (grant Nos 90101020, 10023001 and 10174035). This work was also partly supported by the NPTND of Korea MOST.

References

[1] Canham L T 1990 *Appl. Phys. Lett.* **57** 1046
[2] Ishikawa Y, Shibata N and Fukatsu S 1996 *Appl. Phys. Lett.* **69** 3381
[3] Photopoulos P, Nassiopoulou A G, Kouvatsos D N and Travlos A 2000 *Appl. Phys. Lett.* **76** 3588
[4] Averboukh B and Qin G G 2002 *J. Appl. Phys.* **92** 3564
[5] Chen K J, Huang X F, Xu J and Feng D 1992 *Appl. Phys. Lett.* **61** 2069
[6] Tsybeskov L, Hirschman K D, Duttagupta S P, Zacharias M, Fauchet P M, McCaffrey J P and Lockwood D J 1998 *Appl. Phys. Lett.* **72** 43
[7] Wang M X, Huang X F, Xu J, Li W, Liu Z G and Chen K J 1998 *Appl. Phys. Lett.* **72** 722
[8] Ma Z Y *et al* 2002 *J. Non-Cryst. Solids* **299–302** 648
[9] Wang Y, Matsuda O, Serikawa T and Murase K 2000 *J. Physique* IV **10** 259
[10] Yue G Z, Lorentzen J D, Lin J, Han D X and Wang Q 1999 *Appl. Phys. Lett.* **75** 492
[11] Veprk S, Sarott F A and Iqbal Z 1987 *Phys. Rev.* B **36** 3344
[12] Viera G, Huet S and Boufendi L 2001 *J. Appl. Phys.* **90** 4175
[13] Campbell I H and Fauchet P M 1986 *Solid State Commun.* **58** 739
[14] Zi J, Büscher H, Falter C, Ludwig W, Zhang K M and Xie X D 1996 *Appl. Phys. Lett.* **69** 200
[15] Zhang L, Chen K, Wang L, Li W, Xu J, Huang X F and Chen K J 2002 *J. Phys.: Condens. Matter* **14** 10083